

Electronic Supplementary Information to an article:

Ca-Al double-substituted strontium hexaferrites with giant coercivity

By Lev A. Trusov, Evgeny A. Gorbachev, Vasily A. Lebedev, Anastasia E. Sleptsova, Ilya V. Roslyakov, Ekaterina S. Kozlyakova, Alexander V. Vasiliev, Robert E. Dinnebier, Martin Jansen and Pavel E. Kazin

Section S1. Sample characterization techniques

Powder X-ray diffraction (XRD) phase analysis of all samples was performed using a Rigaku D/MAX 2500 diffractometer (CuK α radiation).

For crystal structure refinement experiments we used two different devices. The spectra of samples with $x = 3.5$ and $x = 4$ was obtained at a laboratory powder diffractometer in Debye–Scherrer geometry (Stadi P-Diffraktometer, Stoe, Mo K α 1 radiation from primary Ge(111)-Johannson-type monochromator, Mythen 1 K PSD detector). The samples were sealed in a 0.5 mm diameter borosilicate glass capillary (Hilgenberg glass No. 14), which was spun during the measurement. The spectra of samples with $x = 3$ were collected at the beamline ID22 in European Synchrotron Radiation Facility (ESRF, Grenoble, France) in a transmission mode [A. N. Fitch, *J. Res. Natl. Inst. Stand. Technol.*, 2004, **109**, 133]. An X-ray beam with a wavelength 0.1770 Å was used. Samples were sealed in a 1.5 mm diameter kapton spinning capillary. The flat panel Perkin Elmer XRD detector (4096 × 4096 pixels of 100 × 100 μm) installed 0.38 m from the sample position was used for data collection in the q -range up to 30 Å⁻¹. For the following Rietveld refinement radial intensity distributions with a step 0.0049° were calculated. All spectra were taken at room temperature.

The Rietveld refinement was performed with the use of Jana2006 software [V. Petricek, M. Dusek, L. Palatinus, *Z. Kristallogr.*, 2014, **229**, 345.]. Interplanar spacing ranges were 0.51 – 4 Å for synchrotron data and 0.51 – 6.7 Å for MoK α 1 radiation. Background was refined with 12 Chebyshev terms. To describe the peak shape, the modified Pseudo-Voigt function was used. The Lorentzian component was refined with respect to the anisotropic microstrains component in the (0 0 1) direction. The absorbance correction was performed with respect to the refined composition. The overall sum of oxygen atoms occupancies was fixed by restrictions. ADP parameters for all oxygen positions was set to be equal. For Ca-containing samples (Series 2) the sum of Ca and Sr was fixed to be full, and ADP parameters to be equal by the restrictions. For all the samples the restrictions keep the sum of aluminum and iron occupancies to be full and their ADP parameters to be equal for each iron position separately. The synchrotron diffraction data allows to refine the overall aluminum content. The differences between the theoretical and the calculated composition was found to be less than 5%. For the MoK α 1 radiation the aluminum content was fixed to be equal to the theoretical composition.

Scanning electron microscopy (SEM) was performed using a LEO Supra 50 VP microscope. Magnetic data were collected using a Cryogenic S700 and a Quantum Design MPMS 7XL SQUID magnetometers in the fields up to 7 T. Curie temperatures were determined by thermogravimetric analysis in a magnetic field (NdFeB magnet) performed with Perkin Elmer Pyris Diamond instrument.

Section S2. Tables

Table S1. Occupancy factors for Al³⁺ cation in hexaferrite sublattices.

| Series ^a | x | $2a$ | $2b$ | $4f_1$ | $4f_2$ | $12k$ |
|--------------------------|-----|---------|---------|---------|---------|---------|
| 1 | 3 | 0.65(4) | 0.07(4) | 0.07(2) | 0.05(2) | 0.34(2) |
| 2 | | 0.66(2) | 0.08(2) | 0.08(4) | 0.08(5) | 0.35(2) |
| | | | | | | |
| 1 | 3.5 | 0.72(1) | 0.07(1) | 0.12(1) | 0.07(1) | 0.39(1) |
| 2 | | 0.72(2) | 0.08(2) | 0.11(4) | 0.07(4) | 0.39(4) |
| | | | | | | |
| 1 | 4 | 0.76(1) | 0.10(1) | 0.14(2) | 0.10(2) | 0.44(2) |
| 2 | | 0.74(1) | 0.04(1) | 0.17(2) | 0.10(2) | 0.45(2) |
| Sandiumenge ^b | | 0.77(4) | 0.22(4) | 0.19(2) | 0.20(2) | 0.38(2) |

^a SrFe_{12-x}Al_xO₁₉ (Series 1) and Sr_{1-x/12}Ca_{x/12}Fe_{12-x}Al_xO₁₉ (Series 2)
^b F. Sandiumenge, S. Gali, J. Rodriguez, *Mater. Res. Bull.*, 1988, **23**, 685.

Section S3. Figures

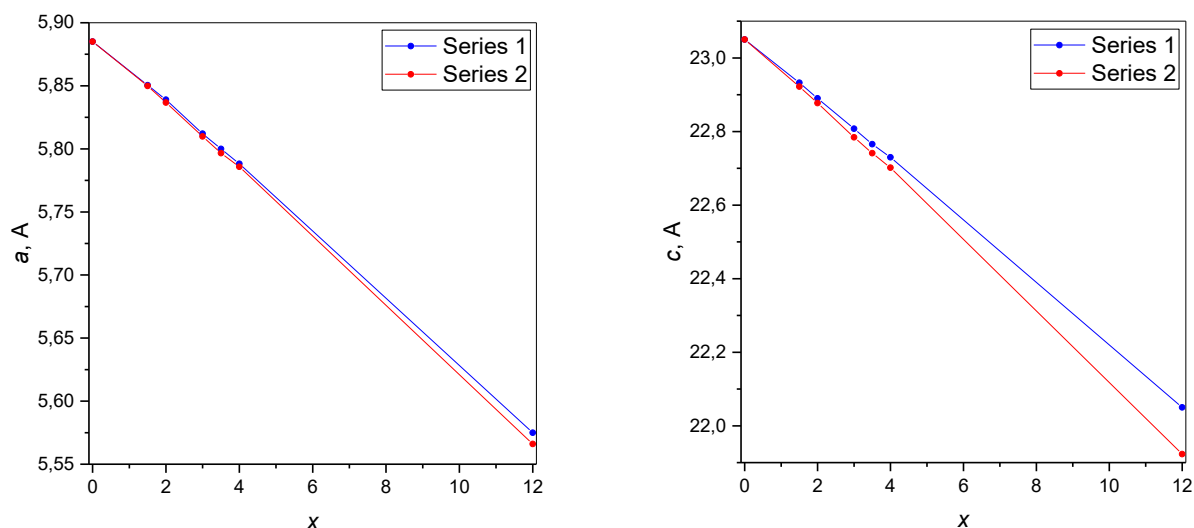


Fig. S1. Lattice parameters of SrFe_{12-x}Al_xO₁₉ (Series 1) and Sr_{1-x/12}Ca_{x/12}Fe_{12-x}Al_xO₁₉ (Series 2) samples. Some parameters were taken from the literature: SrFe₁₂O₁₉ (X. Obradors, et al. *J. Solid State Chem.*, 1988, **72**, 218), SrAl₁₂O₁₉ (Y. Goto, et al. *Jpn. J. Appl. Phys.*, 1973, **12**, 948) and CaAl₁₂O₁₉ (A.M. Hofmeister, et al. *Geochim. Cosmochim. Ac.*, 2004, **68**, 4485).

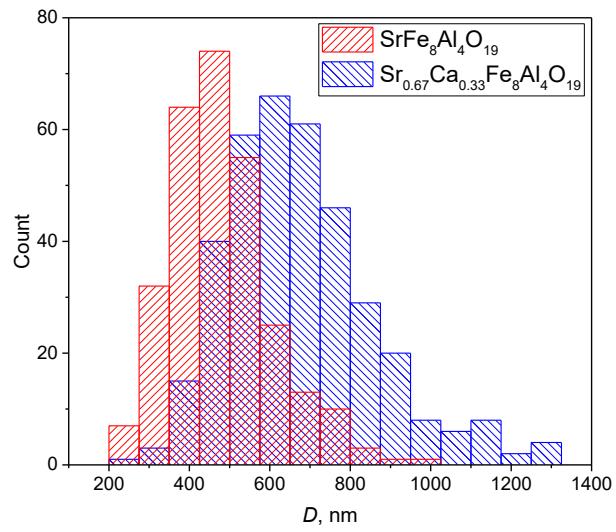


Fig. S2. Particle diameter distributions for $\text{SrFe}_8\text{Al}_4\text{O}_{19}$ (Series 1) and $\text{Sr}_{0.67}\text{Ca}_{0.33}\text{Fe}_8\text{Al}_4\text{O}_{19}$ (Series 2).

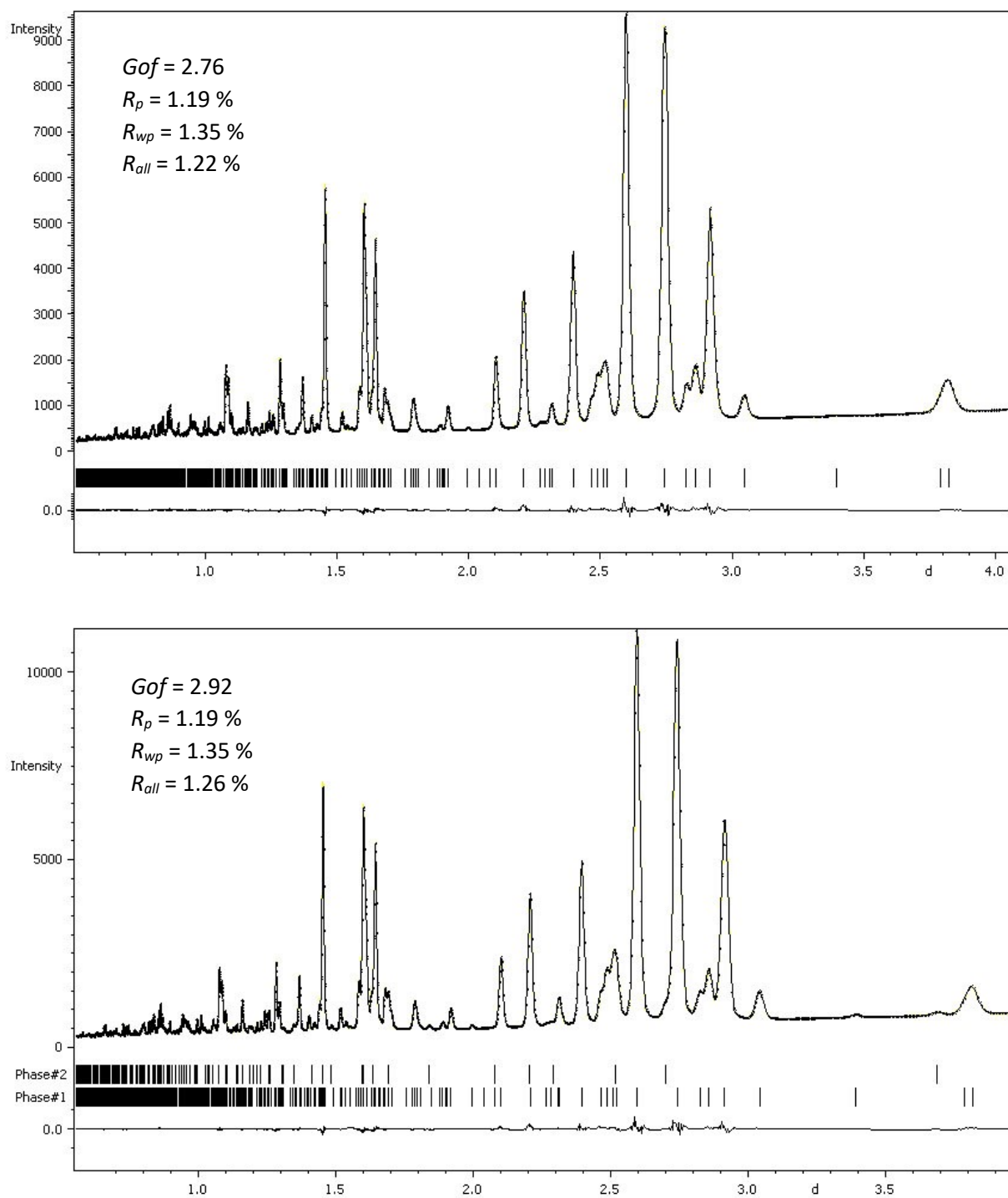


Fig. S3a. Refined synchrotron powder X-ray diffraction patterns of the samples $\text{SrFe}_9\text{Al}_3\text{O}_{19}$ (top) and $\text{Sr}_{0.75}\text{Ca}_{0.25}\text{Fe}_9\text{Al}_3\text{O}_{19}$ (bottom).

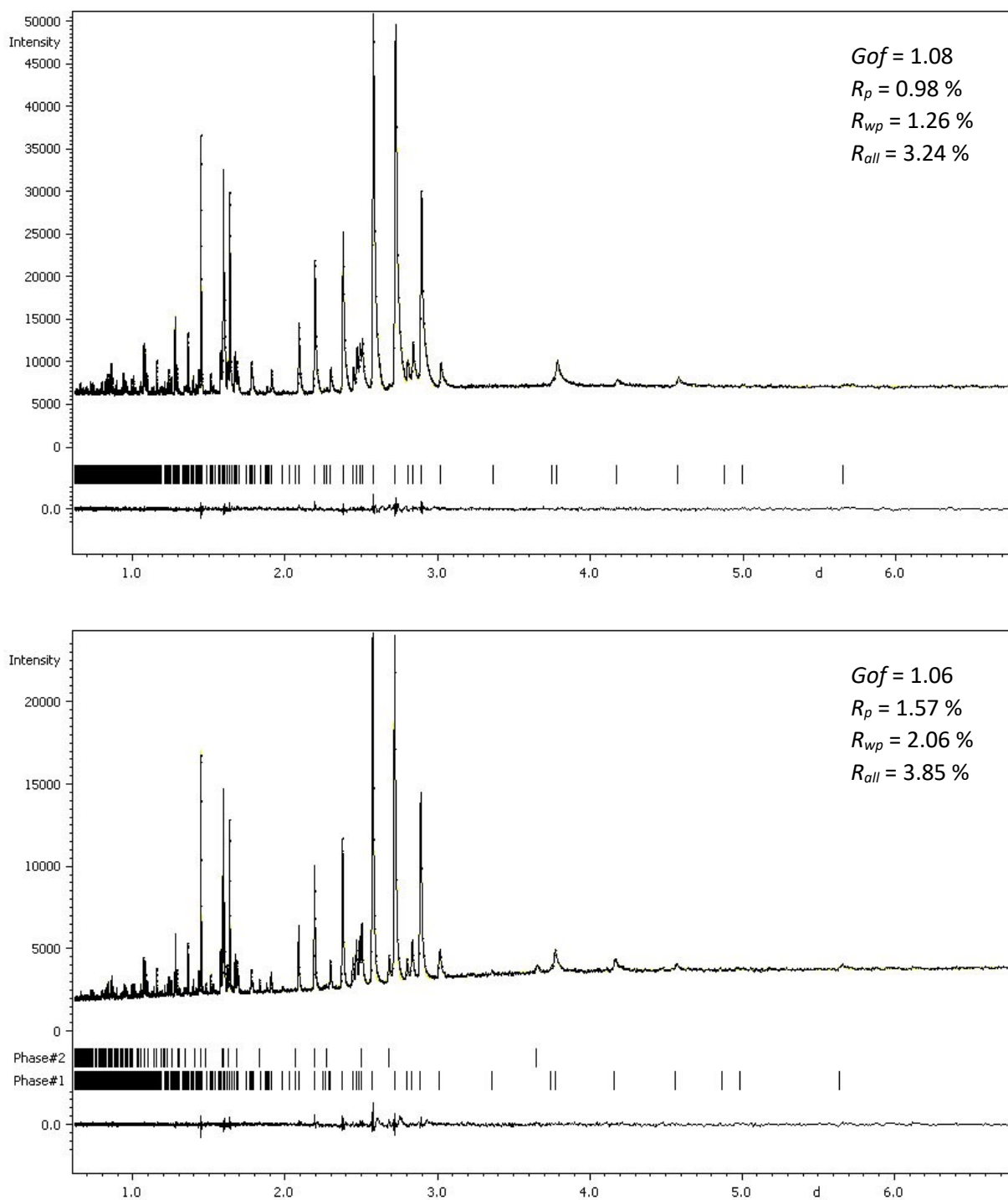


Fig. S3b. Refined powder X-ray diffraction patterns of the samples $\text{SrFe}_{8.5}\text{Al}_{3.5}\text{O}_{19}$ (top) and $\text{Sr}_{0.71}\text{Ca}_{0.29}\text{Fe}_{8.5}\text{Al}_{3.5}\text{O}_{19}$ (bottom).

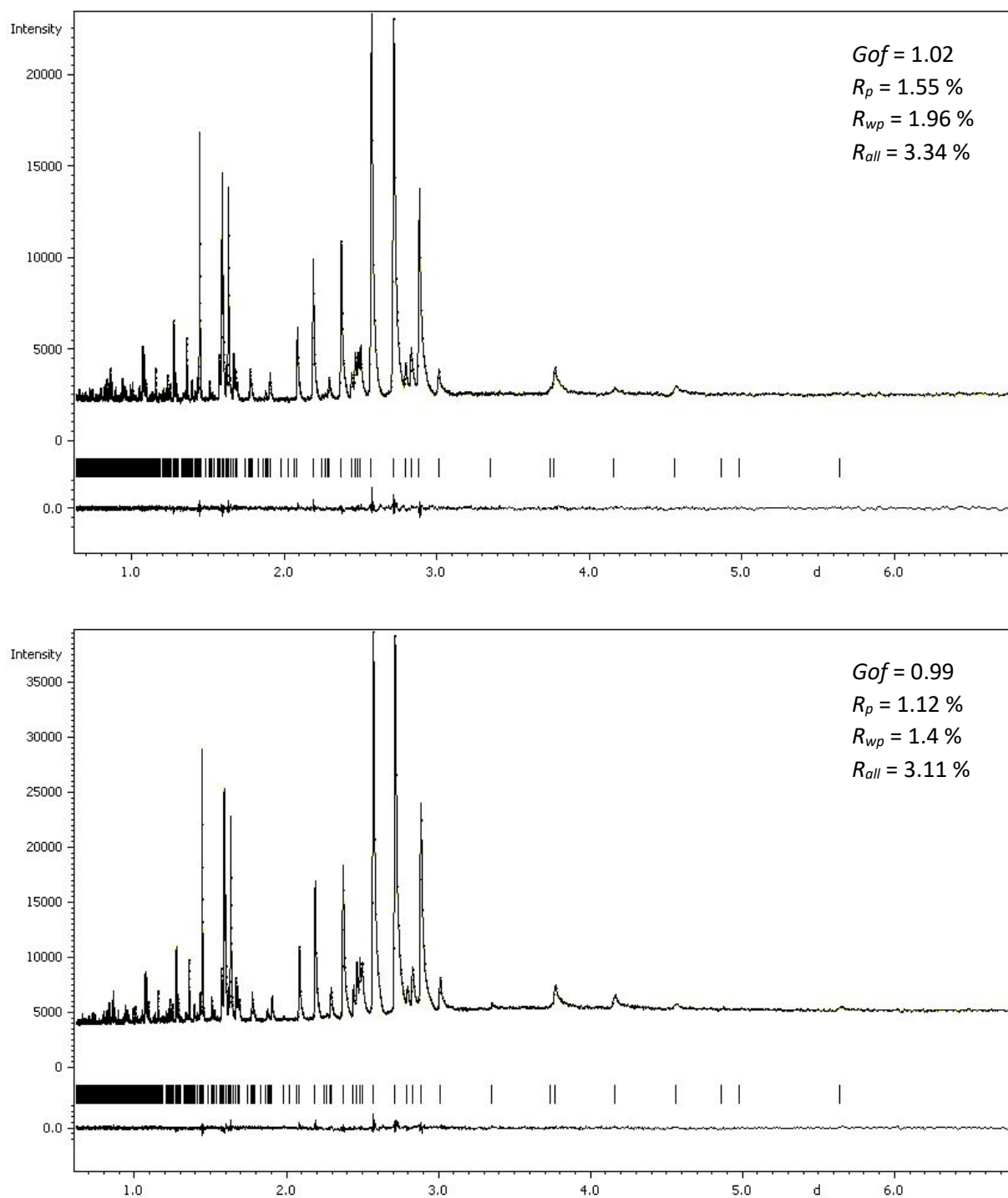


Fig. S3c. Refined powder X-ray diffraction patterns of the samples $\text{SrFe}_8\text{Al}_4\text{O}_{19}$ (top) and $\text{Sr}_{0.67}\text{Ca}_{0.33}\text{Fe}_8\text{Al}_4\text{O}_{19}$ (bottom).

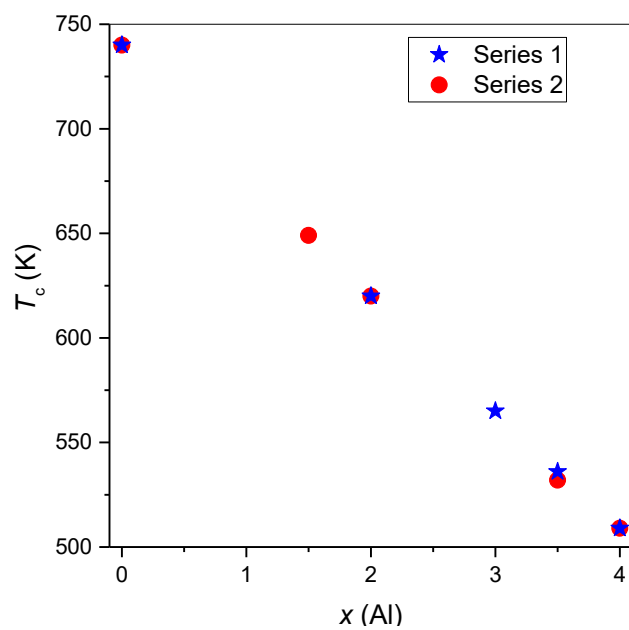


Fig. S4. Curie temperature vs aluminum content plots of $\text{SrFe}_{12-x}\text{Al}_x\text{O}_{19}$ (Series 1) and $\text{Sr}_{1-x/12}\text{Ca}_{x/12}\text{Fe}_{12-x}\text{Al}_x\text{O}_{19}$ (Series 2).